

Reducing Wake in Formula One Cars Using Biomimicry

M.A.D.U.U. Wijetunge
Faculty of Science and Engineering
University of Wolverhampton,
Wolverhampton, United Kingdom
U.U.Wijetunge@wlv.ac.uk

Department of Mechanical and
Automotive Engineering, CINEC
Campus, Millenium Drive, IT Park,
Malabe, Sri Lanka
udithwijetunge53@gmail.com

S. S. G. C. Siriwardana
Department of Mechanical
Engineering, Faculty of Engineering
University of Sri Jayewardenepura,
Nugegoda, Sri Lanka
geethal@sjp.ac.lk

Abstract— This research hopes to find a biomimetic resolution to the wake created in Formula One cars. The turbulent wake created by the Formula One cars in its rear ends have caused a significant satisfaction loss in the sport, due to the lack of overtaking caused by performance loss in a car trailing behind another. Previous methods have been implemented to reduce this effect; however, they show no significant improvement. Biomimetics is an ever-growing field, its multidisciplinary characteristic allows us to combine biologically affirmed designs on our creations to solve problems. The influence of humpback whale tubercles and harbour seal vibrissae were implemented in the rear wings due to their ability to regulate the turbulent air. Numerical simulations were conducted at various speeds for each design including the base model rear wing. The results attained from each design were compared at varying velocities. The biomimetically enhanced models showed an improvement in the wake region when considering parameters like Turbulent Kinetic Energy and Turbulence Intensity. The wake reduction peaked at average Formula One track speeds for each biomimetic alteration. Overall, the study yielded positive results when applying biomimetics. However, the effect of biomimetic enhancements on trailing cars needs to be studied.

Keyword-CFD, Formula One, Wake, Aerodynamics, FIA

I. INTRODUCTION

Formula One cars have undergone vigorous changes over decades, the vehicles are highlighted as the most cutting-edge due to their impressive downforce generation and high speed manoeuvrability. The utilization of inverted wings, diffusers, vortex generators and the overall aerodynamic geometry of the vehicle minimises its drag and maximises the downforce. Race engineers use numerous methods like CFD simulations, wind tunnel testing and on track testing to study airflow characteristics on these vehicles [1]. There is an improved traction, maximisation of tyre loads and adhesion due to high downforce generation [2].

At the early stages of Formula One, aerodynamics was not considered a critical characteristic [3]; most vehicles lacked an aerodynamic design. With rising competition, the importance of aerodynamics became ascertain to the teams [3]. Streamlined bodywork, front wings and spoilers were introduced, the new cars boasted high traction and higher cornering speeds. The facility of CFD in Formula One was

popularised in the 1990s and the sport attracted specialists in fluid dynamics providing a more scientific approach to the development of the vehicles [3]. The 2000s found the turbulent wake to be a problem when a trailing car attempts to overtake a leading car [3]. Modern Formula One cars are optimised to run under free-flow conditions yet, experience a significant loss in performance when exposed to turbulent flows [4]. The wake flow region created by the leading car causes the trailing car in proximity to reduce downforce and drag. Research suggests that the wake mainly affects components like front wing, rear wing and diffuser of the trailing car [4].

The idea of biomimicry is interdisciplinary, it includes the mimicking of plants, animals and biological processes to aid in resolving human problems. Some successes of biomimetic engineering includes influence of kingfisher beaks in bullet train noses to reduce drag and noise [5]. The agility and manoeuvrability of dragon flies were studied and implemented on helicopters [6]. The study of animals and their designs can be integrated into aerodynamic vehicles to diminish the wake region created in the rear [7].

II. LITERATURE REVIEW

A. Prior approaches of Formula One Wake reduction

The earliest technique adapted to resolve the wake problem included ‘The Centreline Downwash Generating Wing’; the idea was proposed to the teams by the FIA in 2005 [8]. The proposed wing design replaced the existing single body rear wings with two box shaped rear wings behind each rear wheel. The middle section was kept empty, and the wings at either end would direct the wake sideways from the car instead of concentrating the wake into the middle, allowing a trailing car to follow behind without losing downforce [7]. The FIA hoped to keep these designs for the 2007 seasons, but the idea was never implemented. The DRS system was implemented to aid in overtaking. This system first emerged in 2011 season; the DRS included a movable flap in the rear wing where the angle was adjustable. Aerodynamic resistance of the vehicle was seen to reduce by 20% when the flap was opened, permitting easier overtaking [3].

In 2022, Formula One had a redesign with major changes to the rules, regulations and design specifications. The 2022 rear wing replaced the flat endplates using a continuous

curved rear wing element consisting of the major dual element rear wing, curved endplates and beam wings. This modification hoped to push the wake upward and outwards from the region which it would affect the rear car. Moreover, the curved transition to the vertical endplates allows the reduction of turbulence created due to the wing [3].



Fig. 1. Rear Wing design under 2022 specifications [9]



Fig. 2. Rear Wing design under 2021 specifications [10].

Complex aero parts like vortex generators and winglets were reduced in the upper body of the car. The underbody of the car used the ‘ground force’- the car’s usual flat underbody is replaced with specially designed air channels to create the venturi effect [3]. An examination of the wake effects of the 2022 specification and 2021 specification rear wings was conducted, the results showed that there was no major reduction in the turbulence produced by the change in the wing design. The results suggests that in the 2021 wing the wake increased and dissipated faster than in the 2022 wing, the rates of dissipation were similar [11]. This data directly disputes the statistics obtained by Pirelli showing a 30% increase in overtakes in the 2022 season compared to the 2021 season [11]. The extracted results do not directly impact the wake generation as the simulations were not conducted on the entire car, only the rear wing [11]. The application of biomimetic designs in Formula One specifically in the goals of reducing wake is novel. While biomimetics have been applied in other fields such as aviation and aerospace, its potential in Formula One is yet to be explored.

B. The effects of Wake on Formula One cars

An analysis was conducted on a 2017 specification Formula One car, it included the simulation of the flow of a leading and trailing car and the extrapolated data shows there are downforce reduction of 23.5%-62% in downforce in a range of vehicle lengths behind the leading car [4]. The abrupt

peaking in aerodynamic loads in the front result in sensitive steering and high possibility of over-steer. This raises safety concerns in high-speed braking situations and sharp corners.

The 2017 specification car has a weight distribution of 45.5% in the front axle and the car tends to increase this value due to the movement of centre of pressure of the car ahead of the centre of gravity of the car [4]. The effects of downforce reduction occur starting at one car length behind the leading car and the reduction in downforce in the front wing peaks at a 38% downforce reduction[4]. Reduction in downforce in the rear wing is vividly observable, this is observable earliest at two car lengths distance behind the leading car. The loss of downforce peaks at 53.3% at 0.25 lengths of a car, under freestream regimes the streamlines are observed to move in an aligned manner, nevertheless, as subjected to wake flows the streamlines are directed to the centre of the rear wings and there is uneven distribution of airflow over the rear wings. Due to the low aspect ratio of the rear wings, it is evident that the rear wings are more susceptible to the direction of the air flow compared to the front wing [4]. The diffuser is observed to be affected the most negatively due to the wake, a 70% loss in downforce and 57% loss in drag is present under proximity of leading car [4].

TABLE I. PERCENTAGE OF CHANGE OF THE AERODYNAMIC COEFFICIENTS IN THE REAR WING OF THE FIRST CAR AS REGARDS TO SECOND CAR [4].

Distance Rear Wing	$SC_L(m^2)$	$SC_D(m^2)$
0.25 Car Length	-57.90%	-53.30%
0.5 Car Length	-54.80%	-50.60%
1 Car Length	-52%	-48%
2 Car Length	-40.30%	-36.20%

Under freestream flows, the airflow under the body is guided through the front wing and vortex generators, showing an aligned flow through the underbody till the diffuser. As the proximity increases, the flow through the underbody reaches at a more disturbed state at the diffuser, reducing its performance. The underbody is situated much lower than the front wing so, it is more sensitive to the wake flows compared to the front wing. The low energy vortical flows are not compresses enough at the under body, being a major causality of reduced downforce.

According to results based on early 1990s Formula One cars, trailing cars saw a downforce reduction of 36% and an aerodynamic drag reduction of 23%[12]. In the mid to late 2000s, trailing cars showed a downforce reduction of 17% and drag reduction of 10%[13]. The reduced drag allows an enhanced straight-line speed which is beneficial in overtaking, commonly known as slipstreaming or drafting[12], [13]. Nevertheless, the reductions of downforce are mainly observed in the front axle, causing front end aero-balance loss of up to 22%. This shift in balance results in understeer, which produces more tyre wear and reduced cornering velocities[14], [15].

In 2017 an experiment was conducted to determine the effects of wake flows on Formula One cars. This experiment used a wake generator (the rear wing and wheel section of a Formula One car) in front of the Formula Car model. At one car length behind the wake generator the front wheel aero balance was reduced up to 11%. The exposed wheels of the trailing car

contribute to a significant vehicle drag of 35% whilst generating a positive lift. In contrast to other studies, the front wing is showed to be least effected by the leading car, mainly observable in front wing drag $\Delta C_D = -0.006$. Alternatively, the rear wing experiences the greatest loss -0.182 in $-C_L$. The greatest losses in downforce are observed when the vehicles are aligned along their centre plane with the reduction of downforce increasing with reduced separation. At proximal ranges the aero balance was reduced to 20% being a significant causality in understeer. The drag and downforce values tend towards the baseline (free stream) values with a small $y = 0.25W$ lateral offset; downforce deficits were almost half of the values obtained at the longitudinal positions, with increases of approximately 0.1 observed in C_D . [15], [16]

At a separation of $0.4L_C$ (closest overtaking spacing) the vehicle experiences 60% loss in C_L and at all wake generator positions the C_L is affected more than C_D . The centre of pressure shifts rearwards, backwards 27% length of wheelbase compared to the free stream results, causing severe understeer and excessive tyre wear. The front wing downforce and (L/D) efficiency is substantially affected by the wake. Moreover, in comparison to the front wing the rear wing and underfloor experience a severe downforce reduction.[15]

C. Parameters used to quantify Wake characteristics in Formula One

Research conducted on the wake flows of Formula One cars; observed parameters like stagnation pressure, velocity and dynamic pressure contours. The contours were numerically and visually analysed to understand structures in wake in the rear of the car [16]. A study conducted in 2013, used Laser Doppler Anemometry (LDA) to make velocity measurements in the proximity of the front wheel of a car, using in-plane velocity data extracted, the Line Integral Convolution (LIC) was adapted to enhance visualization of the vector fields in the wake structure. Moreover, another parameter discussed in the research included the contours of TI in the wake region [17]. In an alternative paper, it was mentioned that the total Coefficient of Pressure (C_p) was a common parameter used to examine complex wake profiles in Formula One; C_p is a non-dimensional parameter relating to the energy of the wake flow relative to the car [18]. A study in 2021 investigated how the wake of an upstream car effects the performance of the trailing car, and these included the analysis of trailing vorticities, velocity deficits in the wake. The TI were visualised at the rear end and sampling of static pressure coefficients, stagnation pressure coefficients and velocity contours were included [19]. Studies were specifically conducted to analyse wake flow patterns, in such experimental investigation the ‘smoke visualization’ of a rear wing was conducted, the overall TI contours were also analysed in this study[20].

D. Reduction of Turbulence using Biomimicry

The use of tubercles as lift enhancement devices aged back to 1995, early research saw that these designs can delay the stall in the wings and increase the overall Lift Coefficient (C_L) [21].



Fig. 3. Smoke visualisation over the rear wing for the design case, vertical elevation with flow moving from bottom to top [20].

The design was implemented in leading edges of wings, the design comprised of a set of patterned peaks and troughs; it was observed that there were large vortices formed in the troughs that resulted in delayed flow separation in the trailing edge. Further research was conducted on hydrodynamic tubercles reduction in tubercles involved a 3-D pair of counter-rotating vortices in the leading edge, the vortices are formed in the peaks of the tubercles and follow a streamwise direction. The vortices are causality of pressure differences in the pressure and suction sides of the foil, resulting in the mixing of the upper and lower boundary layers. The investigation involved a novel energy saving device (ESD) using the biomimetics of tubercles positioned in the rear end of the ship’s hull right ahead of the turbine. Nominal wake axial velocity plots were made at the front of the turbine, the results show that the ship with the ESD had reduced velocity contours and attained the free stream velocity in comparison to the normal ship. Overall, a significant reduction in wake structure was observed at the turbine due to the ESD [21]. Another investigation focused on improving wing performance by adapting the tubercle design. The wake was observed to narrow down and dissipate much earlier in comparison to the normal wing [22]. A 2021 study included the analysis of using leading edge tubercles in aerospace applications for flow control. For this simulation the shear stress transport $k-\omega$ turbulence model was adapted on an aircraft wing profile. When observing the velocity streamline field patterns in the normal wing profile and the trough and peak regions of the biomimetic tubercle profile; the peaks showed a delay in wake formulation, the trailing wake region was also minimised. In comparison to the normal wing the troughs also have a reduced wake. Due to the strength of the vortex generated, there occurs a significant momentum exchange in the flow causing the flow separation to be delayed in the peak regions [23], [24].

III. METHODOLOGY

This study includes the numerical simulation of a Rear Wing of a Formula One car considering its role in wake management [4]. The 2-D simulations across three planes of the full Formula One car [25] under the standards of FIA 2022 regulation was conducted at three selected velocities, this helped set accurate inlet properties for the 3-D simulation of the rear wing. Biomimetic alterations were made, based on

literature, to the base rear wing and the effect of Biomimicry in wake reduction was studied. Using the parameters selected through literature, the reduction of wake region was observed visually and numerically. For this study, ANSYS Fluent @ was used to solve RANS simulations and the $k-\omega$ Turbulence Model was selected as it delivered faster convergence and is suitable for similar external flow simulations, the model uses $k-\epsilon$ model for far field regions and switch to $k-\omega$ near boundary layers [26] [27]. Both the car's 2D profiles and rear wing was simulated for 54, 180 and 324 kmh^{-1} , for flows in sharp corners, average speeds and high speed straights respectively[28] .

A. Mesh Generation

A grid convergence test was carried out to determine the accuracy of the mesh used for the simulation. The figure shows the variation of the results obtained for varying mesh sizes. The difference between percentage values obtained for each mesh was below 1%. The 50 mm tetrahedral mesh was used throughout the entire study considering both times taken for simulations and accuracy of computation in comparison the three cases. Each of the meshes were given an inflation on the rear wing with a first layer thickness of 1 mm and 5 layers. Since the rear wing is symmetric, the enclosure was created for half of the rear wing, and the study was conducted for half of the rear wing considering the computational power limitations and accuracy.

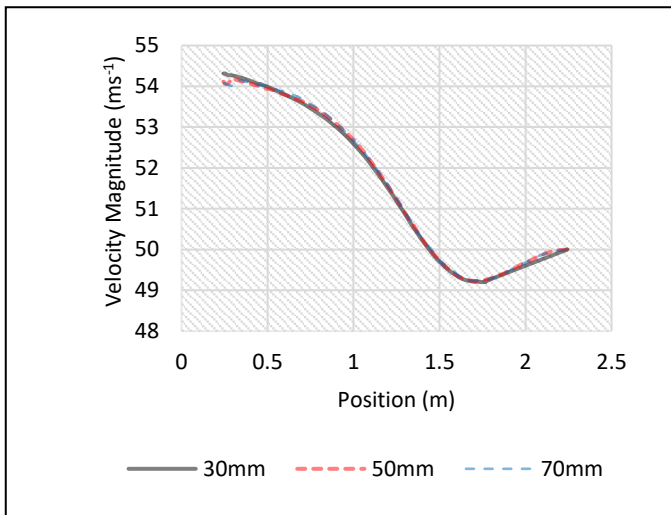


Fig. 4. Velocity Distribution across a longitudinal line in the enclosure.

Research conducted in 2023 quantified the impacts of the 2022 regulations, comparing the 2021 specification rear wing with the 2022 specification rear wing [11]. In the streamline plots the 2021 specification rear wing showed a premature detachment of the air in the centre plane, whereas the 2022 specification rear wing showed a delay in detachment [11]. A larger vortex is observed in the 2021 specification rear wing. Conversely, the 2022 specification lacks this vortex, and a similar flow pattern can be visualized in the mid plane of 2022 rear wing model used in the CFD analysis. This suggests that the 2022 model used in the current CFD analysis captures the overall flow pattern in a 2022 Rear Wing.

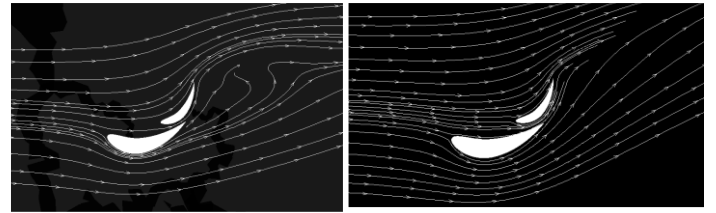


Fig. 5. (Left) Streamline plots at Centre Plane for 2021 rear wing[11]. (Right) 2022 Rear Wing[11].

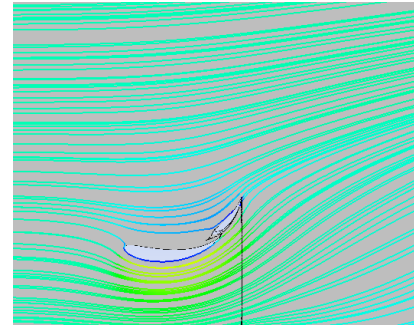


Fig. 6. Streamline for current 2022 Rear Wing at Centre Plane.

B. Geometry

The rear wing [25] consists of two endplates with a flat cross section and a dual element wing. The length of the rear wing L is 0.4 m, its height H is 0.6 m and the maximum width of wing W is 1.27 m.

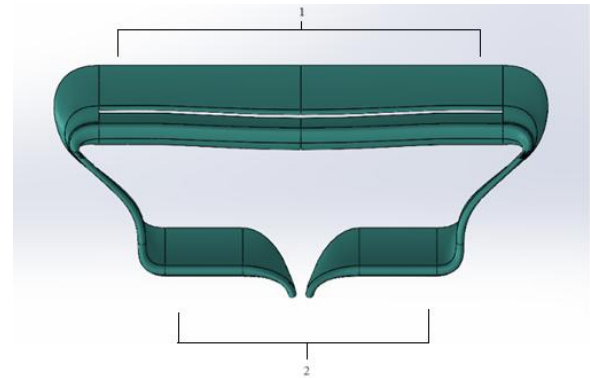


Fig. 7. Section 1 and section 2 of the rear wing.

This study consists of the comparison of the base rear wing and three other bio-inspired designs: BIO-1, BIO-2 and BIO-3. BIO-1 combined the designs of the leading-edge tubercles and trailing edge design of harbour seal vibrissae. These were applied to both the main and DRS flap in section 1 of the rear wing. BIO-2 used the design of leading-edge tubercles and applied it on the main and DRS flap on section 1 and at section 2. BIO-3 combined the use of leading-edge tubercles and trailing edge harbour seal vibrissae design; these designs were applied on section 1 main flap and section 2 of the rear wing.

C. Geometry

The boundary conditions for the 2D simulations of the full car was set as follows:

TABLE II. BOUNDARY CONDITIONS FOR 2D SIMULATIONS

Case No.	1	2	3
Velocity Inlet (ms^{-1})	15	50	90
TI at Inlet (%)	0.15[4]	0.15[4]	0.15[4]
Pressure Outlet	1 atm	1 atm	1 atm

The symmetry condition was applied to the top edge, no-slip stationary wall was applied to the car and no-slip moving wall at the respective speed was applied to the floor. 2D simulations were run for three planes: midplane, 0.30 m from midplane and 0.40 m from midplane. The 2D simulation was conducted to predict the inlet conditions for the 3D simulations; the inlet lies 0.4 m ahead of the rear wing so the values for velocity and TKE were obtained. The TI was calculated using the following equation:

$$k = \frac{3}{2}(IU)^2 \quad (1)$$

TABLE III. VALUES CALCULATED AT 15MS⁻¹

Distance From Midplane	Velocity (ms^{-1})	TKE(Jkg^{-1})
0.00m	14.3342	2.573500
0.30m	12.8773	0.409014
0.40m	12.8096	0.242285

TABLE IV. VALUES CALCULATED AT 50MS⁻¹

Distance From Midplane	Velocity(ms^{-1})	TKE(Jkg^{-1})
0.00m	47.5831	28.3088
0.30m	42.7250	4.9450
0.40m	45.3083	3.4415

TABLE V. VALUES CALCULATED AT 90MS⁻¹

Distance From Midplane	Velocity(ms^{-1})	TKE(Jkg^{-1})
0.00m	97.5831	99.5640
0.30m	76.9085	16.2381
0.40m	81.5413	10.8934

Symmetry conditions were given to the Midplane of the rear wing and the faces of enclosure representing the atmosphere- the top and side faces.

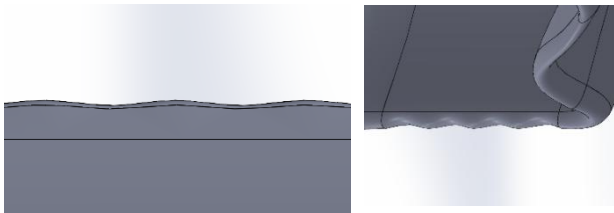


Fig. 8. (Left) Trailing edge Harbor Seal Vibrissa design; (Right) Leading Edge Tubercles.

TABLE VI. BOUNDARY CONDITIONS FOR 3D SIMULATIONS

Velocity Inlet (ms^{-1})	13.34036667	42.23183333	85.3443
TI Inlet %	6.345632909	6.308758312	6.217271278
Pressure Outlet	1 atm	1atm	1 atm
Floor Speed Moving Wall (ms^{-1})	15	50	90

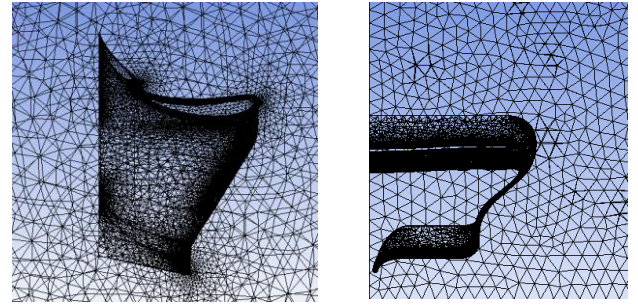


Fig. 9. Tetrahedral Mesh used in 3D simulations.

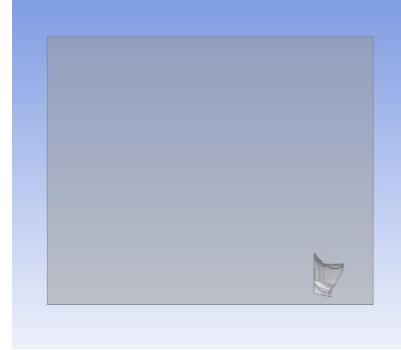


Fig. 10. Enclosure used in 3D simulations.

IV. RESULTS AND DISCUSSION

The results and observations from the numerical simulations conducted are presented in this section. The results are divided into the different velocities that the simulations were run in. Furthermore, the parameters studied in previous literature like TKE, TI, Vorticity and velocity profiles are utilised to study the wake region.

A. Simulations at 15ms⁻¹

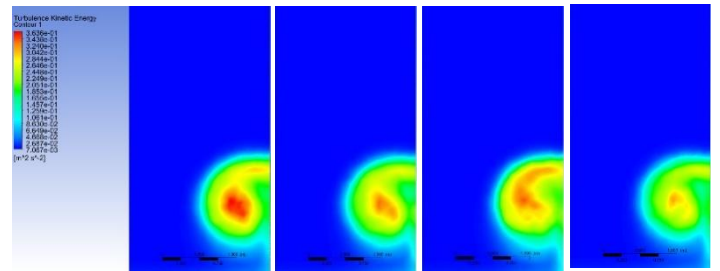


Fig. 11. TKE Contours 3.6m behind the Rear Wing (Left to right: Base, BIO-1, BIO-2 and BIO-3).

The TKE contours in Fig. 11. Transverse planes allow us to determine the differences in wake formulation in each design. This transverse plane study illustrates the variation in the overall width of the wake. The contour shows a circular vortex created with the magnitude peaking at its centre BIO-1 and BIO-3 show an overall reduction in TKE in this plane. However, BIO-2 shows an increase in TKE in comparison to the base wing. This suggests that BIO-2 shows no efficiency in terms of wake regulation in low velocities. Overall, BIO-3 shows the greatest wake reduction with a 15% reduction in TKE compared to the base wing. The position of the vortex

centre can directly affect the front wing performance of the trailing car due to its position, thereby from the results attained above, BIO-3 shows a greater diminishing of wake region allowing improved performance of a trailing car. The average vorticity calculated at each transverse plane shows an overall reduction for the biomimetic wings. The greatest reduction in vorticity is seen in BIO-2 however. This suggests that despite the reduction in rotational frequency, the overall fluctuations in velocity in the wake of BIO-2 are greater in comparison to the other wings.

B. Simulations at 50ms^{-1}

Fig. 12 shows the TKE contours 0.20m from the center plane. The longitudinal planes allow an alternative visualization of the development of the wake. The turbulent air starts off narrow and maximizes towards the outlet. Both the beam wing and main wing are responsible for the wake created, with the beam wing generating most of the wake. When comparing the base wing with BIO-1 in Fig. 12 the flow separation at the trailing edge shows a reduction. The application of biomimetics to section 2 (beam wing) of the rear wing in BIO-2 and BIO-3 shows a suppressed wake region created with BIO-3 showing the greatest reduction. The narrowing down of these wake regions suggests that the effect it will have on the trailing car is minimized, in BIO-2 and BIO-3 the initial wake region is suppressed greatly, this suggests that even in proximal conditions the trailing car will be able to retain its aerodynamic efficiency.

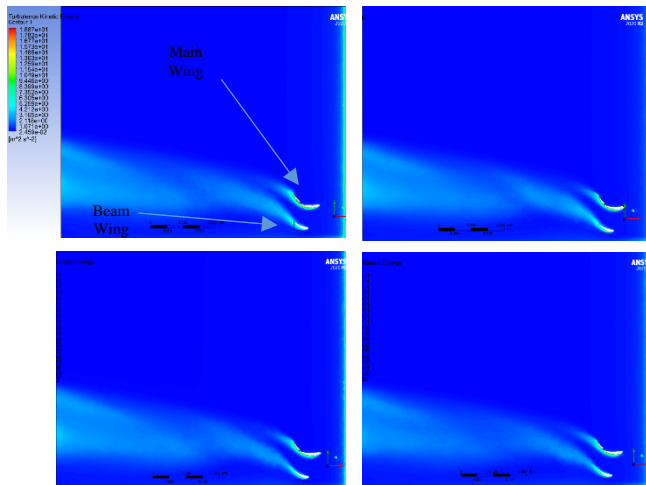


Fig. 12. TKE Contours 0.20m from the Center Plane of Rear Wing. (Clockwise from top left: Base, BIO-1, BIO-3 and BIO-2).

In Fig. 13 the variation of average TKE measured at three transverse planes is observed. The average TKE begins at a low magnitude near the rear wing with its magnitude suddenly increasing at around 2.4m behind the wing. BIO-1 is initially composed of an average TKE greater than the base wing, it gradually shows a reduction in comparison to the base wing. BIO-2 and BIO-3 start off with lower average TKE values, BIO-2 loses its efficiency with length behind the rear wing and shows an increase in TKE in comparison BIO-3. BIO-3 maintains a reduced average TKE throughout the distance and can be considered the best biomimetic design in this scenario.

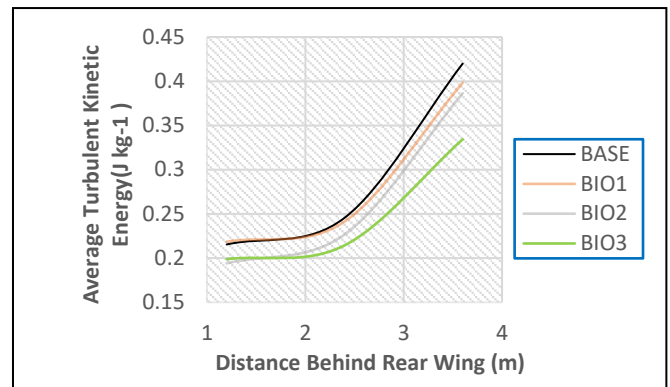


Fig. 13. Variation of average TKE with distance.

Fig. 14 shows the Turbulence Intensity contours 3.6m behind the rear wing. The contours show a similar vortex shape to that of the TKE contours. The reddish regions at the center of the vortex imply the greatest magnitude of TI, BIO-3 shows the greatest diminishing of this reddish region, with BIO-2 and BIO-1 showing minor improvements in comparison to the base rear wing. The vortex region in BIO-3 shows a quicker shift from red to green from the middle of the vortex in comparison to all other designs. This means that the development of the turbulent energy from the centre of the vortex is quickly dissipated. This reduction in vortex strength allows the trailing car to sustain its control without sudden steering sensitivity increases.

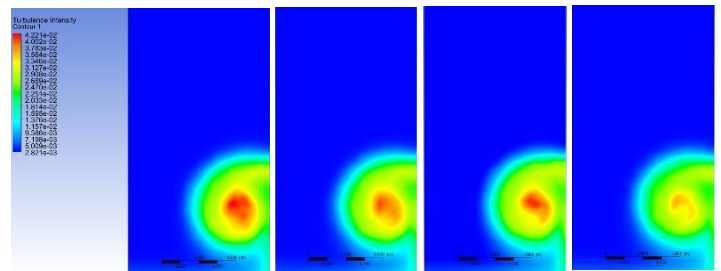


Fig. 14. TI Contours 3.6m behind the Rear Wing (From Left to Right: Baseline, BIO-1, BIO-2 and BIO-3).

C. Simulations at 90ms^{-1}

Fig. 15 presents the TKE contours on a transverse plane located 1.2m behind the rear wing. At this position the vortex is smaller in comparison to further downstream, suggesting that the vortex widens with increasing length. Among the biomimetic wings BIO-3 presents a reduction in TKE magnitude while BIO-1 and BIO-2 demonstrate an increase in TKE particularly at the vortex core. Prior literature suggested that design inspirations with tubercles and harbour seal vibrissae displayed an accelerated development and dissipation of the overall wake, which could explain the greater initial TKE in BIO-1 and BIO-2 in comparison to the base rear wing. Nevertheless, BIO-3 manages to contradict the above trend by sustaining a lower average TKE in the plane in comparison to the Base Wing. Suggests that certain biomimetic designs can help reduce the wake formulation throughout a certain length in comparison to conventional rear wings. It also implies that a more in-depth study of various biomimetic iterations can help identify in which

positions of the model will biomimetic alterations yield best results.

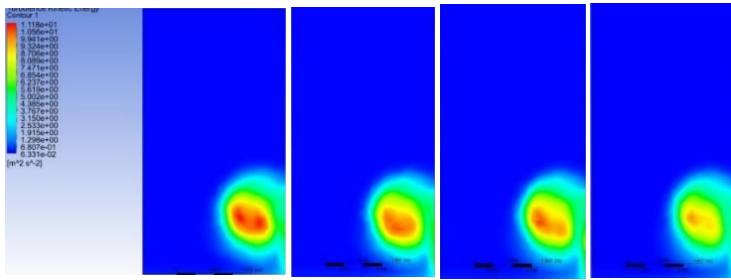


Fig. 15. TKE 2.4 m behind the Rear Wing (From left: Baseline, BIO-1, BIO-2 and BIO-3).

In Fig. 16 illustrates that the greatest magnitude of TKE is at the centre of the vortical structure. Compared to the Base rear wing, all biomimetic wings have demonstrated a reduction in TKE magnitude, with BIO-3 showing significant improvement over BIO-1 and BIO-2. The overall turbulence strength is reduced at the wake's center region whilst, the overall size of wake remains unchanged. When compared to the wake improvements at 15 ms⁻¹ and 50 ms⁻¹ Fig. 16 shows only a minor improvement in the wake region suggesting that at higher velocities the effectiveness of biomimetic wings reduce.

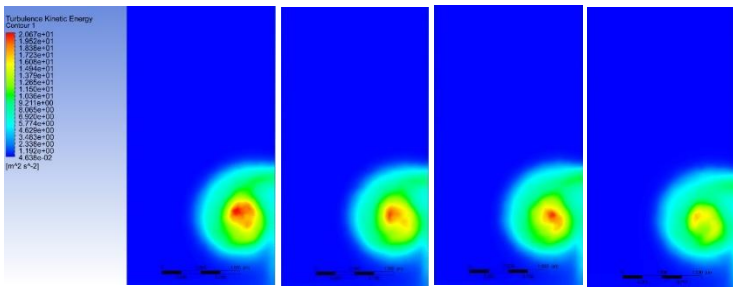


Fig. 16. TKE Contours 3.6m behind the Rear Wing (From left: Baseline, BIO-1, BIO-2 and BIO-3).

TABLE VII. AVERAGE MAGNITUDE OF VORTICITY ACROSS TRANSVERSE PLANES.

Distance behind Rear Wing (m)	Base (Hz)	BIO-1(Hz)	BIO-2 (Hz)	BIO-3 (Hz)
1.2	24.5439	25.6626	25.5538	24.2791
2.4	25.3391	25.4211	25.7617	25.0938
3.6	30.2359	29.7729	30.398	29.403

The average magnitude of vorticity across transverse planes behind the rear wing were analyzed. Initially, BIO-1 and BIO-2 exhibit a vorticity magnitude greater than the base model. However, the magnitude of vorticity reduces with distance for BIO-1 and towards 3.6m it displays an overall reduced vorticity in comparison to the base rear wing. BIO-3 consistently displays reduced vorticity across all planes relative to the base model. Despite the improvements in other wings, BIO-2 maintains a higher vorticity than the base throughout the length. The results for BIO-3 in Table. VII

shows an overall reduction in vorticity in comparison to the base wing, supporting the hypothesis in which biomimetic design can be utilized to regulate wake created in cars.

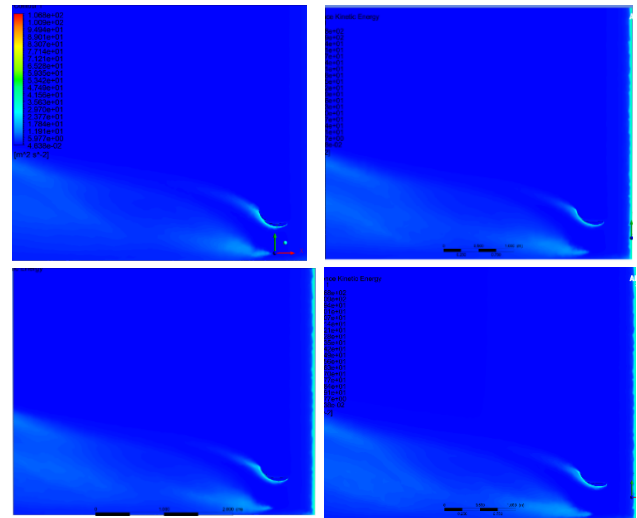


Fig. 17. TKE contours at the centre plane of the rear wing at 90 ms⁻¹. (Clockwise from top left: Baseline, BIO-1, BIO-3 and BIO-2).

Fig. 17 shows the TKE contours at the centre plane, where the flow separation near the main wing (section 1) is noticeably diminished in the biomimetic wings, particularly BIO-1 and BIO-3. Both wings incorporate the use of the harbour Seal Vibrissae design in the trailing edge which appears to suppress the separation at the trailing edge of the flap. Biomimetic features were applied at section 2 for BIO-2 and BIO-3, the wake observed in section 2 of BIO-3 is slightly narrower in comparison with the other wings. However, towards the outlet the overall turbulence levels appear analogous, indicating a consistency in wake region size. However, the areas of high turbulence magnitudes within the wake region in transverse planes is reduced.

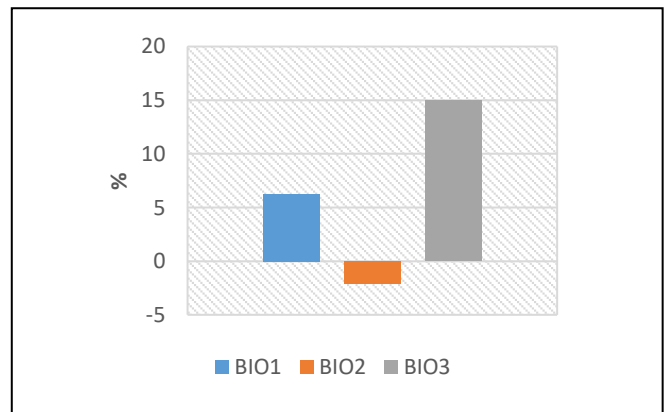


Fig. 18. Efficiency of Biomimetic wings in terms of TKE at 15ms⁻¹.

D. Streamlines on Rear Wing

Wall shear streamlines were used to examine the flow patterns on the surface of rear wing. As shown in Fig. 20 the streamlines run straight from the leading to the trailing edge along the center of the main flap. Nevertheless, towards the edges, the airflow from the leading edge moves laterally towards the side plates and escapes from the rear wing's edge.

At the rear-view Fig. 21 the air that converges at the endplate edges and main wings show a creation of vortices, contributing to the main swirling vortices behind the rear wing [29]. It can be assumed that regulation of formulation of these vortices the overall vorticity behind the rear wing can be controlled. In fact, the regulation change from 2021 to 2022 specifications [3] were to reduce the formulation of these wing tip vortices.

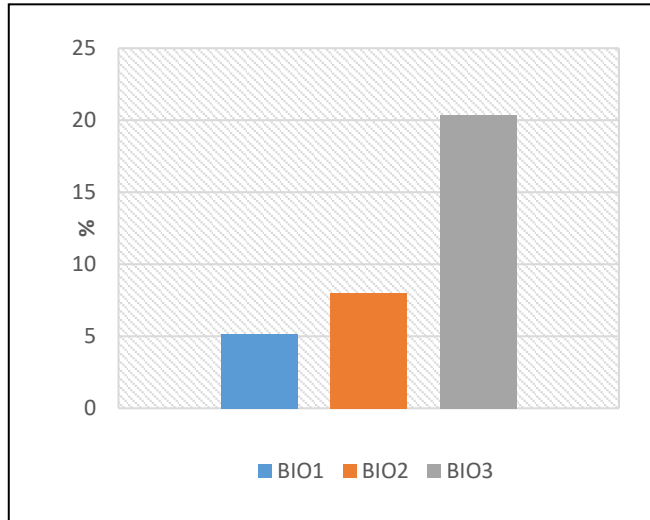


Fig. 19. Efficiency of Biomimetic wings in terms of TKE at 50ms^{-1} .

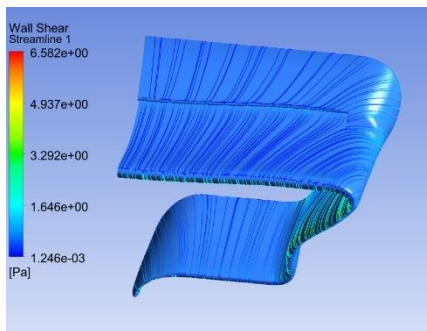


Fig. 20. Surface streamlines of wall shear on base rear wing at 15ms^{-1} front view.

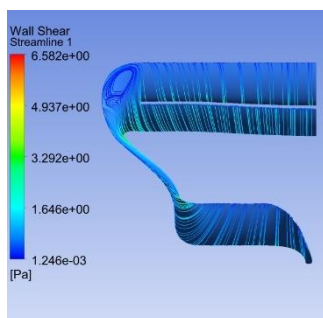


Fig. 21. Surface streamlines of wall shear on base rear wing at 15ms^{-1} rear view.

Fig. 22 illustrates the variation of the vortex formed at the wingtip. At BIO-1 and BIO-3, the vortex moves towards the outer edge of the curve that connects the endplate to the main wing, whilst in BIO-2 this vortex is formed closer to the main flap at the upper edge of the curve. The shift of vortex

observed in BIO-1 and BIO-3 is likely due to the presence of the trailing edge harbour seal vibrissae design.

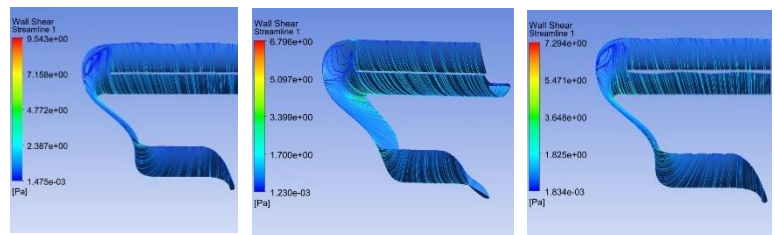


Fig. 22. Surface streamlines of wall shear at 15ms^{-1} (From left: BIO-1, BIO-2 and BIO-3).

Moreover, the streamlines on the main flap appear more disoriented in BIO-1 and BIO-3 influenced by the biomimetic design, whereas BIO-2 exhibits smoother undisturbed flow. At greater velocities, the wing tip vortices on the surface tend to dissipate, this is likely due to the vortices forming closer to the outer edge of the wingtip at greater velocities. Through the alteration of where the wing tip vortex forms in the surface the overall intensity and wake width can be reduced. The observed disordered flow patterns in BIO-1 and BIO-3 can potentially aid in lowering the trailing edge vortices intensity. Through such minimization not only can the drag of the car be reduced but also the aerodynamic efficiency of the trailing car can be improved.

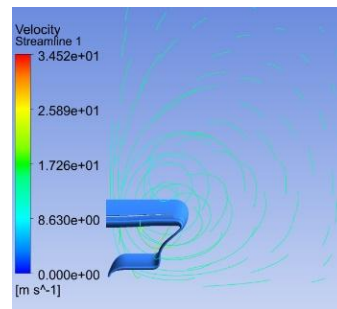


Fig. 23. Velocity streamlines around rear wing at 15ms^{-1} front view.

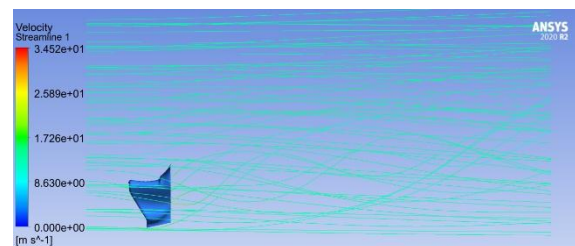


Fig. 24. Velocity streamlines around rear wing at 15ms^{-1} side view.

Fig. 23 and Fig. 24 display the streamlines behind the rear wing, clearly visualizing the main swirling vortices created by the rear wing. These vortices gradually move upwards due to the upwash effect of the rear wing. As the simulation was only run for half of the rear wing, the overall airflow across the full rear wing is symmetric, mirroring the results on the opposite side.

E. Comparisons of Biomimetic Wings

Fig. 18 shows the efficacy of bioimimetic wings in terms of wake reduction at 15ms^{-1} . Overall, the biomimetic wings display limited efficiency at low speeds, with BIO-2 even displaying an increase in wake approximately 3.6 m behind the wing. However, BIO-1 and BIO-3 yields positive results in this scenario, suggesting despite their smaller improvements biomimetic wings will still be beneficial in reducing the wake at low speeds. In Fig. 19 all wings reach peak efficiency in terms of wake regulation with BIO-3 achieving a significant 20% reduction in wake. Given that the peaking of efficiency occurs at the average Formula One speeds it can be inferred that during a significant duration of the race these biomimetic will be effective in minimising wake for a significant duration of the race.

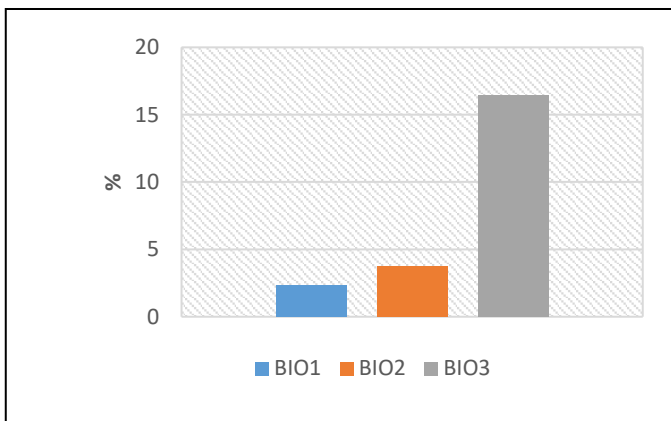


Fig. 25. Efficiency of Biomimetic Wings in terms of TKE at 90ms^{-1} .

Fig. 25 illustrates the efficiency of the biomimetic wings at 90ms^{-1} with their overall performance declining at this scenario in comparison to average Formula One velocities. Despite this reduction, biomimetic continue to perform well at greater velocities in comparison to low velocities. This translates to reduction in drag at higher velocities moreover the reduction of wake at higher velocities reduce safety concerns like downforce loss at high speed corners, and improved steering stability while overtaking at high velocities.

TABLE VIII. EFFICIENCY OF BIOMIMETIC WINGS IN TERMS OF VORTICITY AT DIFFERENT VELOCITIES.

	15ms^{-1}	50ms^{-1}	90ms^{-1}
BIO-1	1.717325%	1.941382%	1.696659%
BIO-2	4.885052%	3.810653%	-0.53612%
BIO-3	2.411411%	4.563753%	2.754672%

All wings exhibit improvements in vorticity across different velocities. However, BIO-2 displays a decline in efficiency with increasing speeds ultimately showing a negative result at 90ms^{-1} . In contrast, other wings obtain peak improvements at 50ms^{-1} again stating that optimal performance is observed at average Formula One speeds. Among all iterations, BIO-3 provides the best performance in terms of wake regulation, supported by the parameters discussed in this research.

V. CONCLUSION

The investigation was carried out to determine if Biomimicry can be implemented to reduce the wake produced in Formula One cars. This study compared a base rear wing with three bio-inspired designs with the studies carried out at three velocities. The results from simulations imply that the biomimetic renditions effectively reduced the wake, with BIO-3 achieving the most prominent reductions in parameters like TKE and TI. Most designs reached peak efficiencies at 50ms^{-1} suggesting optimal performance at typical Formula One velocities. The positive outcomes of utilizing bio-inspired designs in wake reduction imply that these wings can perform optimally during the majority of Formula One races. Furthermore, improved wake management can enhance steering sensitivity for trailing cars by providing improved downforce. When biomimicry was applied to section 2 (beam wing) the resulting wake reduction was evident, suggesting that targeted application of biomimetic features can yield even greater results. The careful consideration and observation of flow patterns for various designs is crucial for obtaining exceptional results as lucidly observable in BIO-3. Further research assessing the impact of these improvements on trailing car performance is crucial for extensive validation. Reflectively, the current study's limitation is its lack of 3D simulations of the entire car, which can affect the overall wake structure and its implications.

A. Future Research Directions

Further research is needed to experimentally validate the performance of biomimetic wings in real-world conditions and optimize the designs for varying track scenarios. The results obtained through experimentation like HWA, smoke visualization and wind tunnel testing can be drastically different to the results yielded through CFD validation thus, it remains as an area of improvement for this study. Moreover, since the 3-D simulations were not conducted for the entire Formula One car, this remains as a drawback for this study. The flow structures in the wake are deemed to change when barricaded by the vehicle structure, this can also hinder results obtained in study so a full simulation will be required to further validate the effectiveness of biomimetics in Formula One wake reduction. Reflectively, as the goal is to avoid the performance losses faced by trailing cars, it will be ideal to validate the trailing car performance when trailing behind a biomimetically enhanced leading car. This can verify the positive effects that can occur in terms of aerodynamic performance due to a biomimetically diminished wake structure.

VI. ACKNOWLEDGEMENT

The researchers express their gratitude towards CINEC campus, for providing access to the computer facilities significant for conducting the simulations and analyses required for completion of this study.

TABLE IX. SYMBOLS

C_L -Lift Coefficient
C_D -Drag Coefficient
C_p - Pressure Coefficient
k- Turbulent Kinetic Energy
I – Turbulence Intensity
U- Mean Velocity
L-Lift
D- Drag
CoP- Centre of Pressure

TABLE X. ACRONYMS

CFD- Computational Fluid Dynamics
FIA- Fédération Internationale de l'Automobile
DRS- Drag Reduction System
LIC- Line Integral Convolution
TI- Turbulence Intensity
ESD- Energy Saving Device
LDA- Laser Doppler Anemometry
RANS- Reynold's-Averaged Navier-Stokes Equations

REFERENCES

- [1] J. Katz, 'Aerodynamics of Race Cars', *Annu. Rev. Fluid Mech.*, vol. 38, no. 1, pp. 27–63, Jan. 2006, doi: 10.1146/annurev.fluid.38.050304.092016.
- [2] P. G. Wright, 'Aerodynamics for formula 1', *The Aeronautical Journal (1968)*, vol. 78, pp. 226–230, 1974, [Online]. Available: <https://api.semanticscholar.org/CorpusID:113930647>
- [3] Z. Zhang, 'Study on aerodynamic development in Formula One racing', *TNS*, vol. 14, no. 1, pp. 38–41, Nov. 2023, doi: 10.54254/2753-8818/14/20240875.
- [4] A. Guerrero and R. Castilla, 'Aerodynamic Study of the Wake Effects on a Formula 1 Car', *Energies*, vol. 13, no. 19, p. 5183, Oct. 2020, doi: 10.3390/en13195183.
- [5] '» The Kingfisher and the bullet train – In the news'. Accessed: Mar. 11, 2024. [Online]. Available: <https://gtac.edu.au/the-kingfisher-and-the-bullet-train-in-the-news/>
- [6] J. Usherwood and F.-O. Lehmann, 'Phasing of dragonfly wings can improve aerodynamic efficiency by removing swirl', *Journal of the Royal Society, Interface / the Royal Society*, vol. 5, pp. 1303–7, May 2008, doi: 10.1098/rsif.2008.0124.
- [7] V. Srinivas, 'Biomimicry as a tool for the Aerodynamic Drag Reduction of Class 8 Heavy Vehicle Trailers: A Computational Analysis and Wind Tunnel Study.', vol. 16, no. 3, 2023.
- [8] 'Radical wing to help overtaking', Oct. 24, 2005. Accessed: May 26, 2024. [Online]. Available: http://news.bbc.co.uk/sport2/hi/motorsport/formula_one/4371456.stm
- [9] M. Hughes, 'Tech Tuesday: How the rear wing of the 2022 car has been designed to be an F1 gamechanger | Formula 1®', TECH TUESDAY: How the rear wing of the 2022 car has been designed to be an F1 gamechanger. Accessed: Aug. 22, 2024. [Online]. Available: <https://www.formula1.com/en/latest/article/tech-tuesday-how-the-rear-wing-of-the-2022-car-has-been-designed-to-be-an-f1-70dkHlNyP8DiGDDnMf3tzU>
- [10] M. Hughes, 'Rapid Reaction: Our first tech take on Alfa Romeo's 2021 C41 | Formula 1®', *Rapid Reaction: Our first tech take on Alfa Romeo's 2021 C41*. Accessed: Aug. 22, 2024. [Online]. Available: <https://www.formula1.com/en/latest/article/rapid-reaction-our-first-tech-take-on-alfa-romeos-2021-c41.2upUpnrWYdMZMdXa0wzrQ>
- [11] L. A. Méndez, 'Quantifying the Impact of the 2022 Formula One Technical Regulations on Wake Turbulence: A Numerical Analysis'.
- [12] R. G. Dominy, 'The Influence of Slipstreaming on the Performance of a Grand Prix Racing Car', *Proceedings of the Institution of Mechanical Engineers, Part D: Journal of Automobile Engineering*, vol. 204, no. 1, pp. 35–40, Jan. 1990, doi: 10.1243/PIME_PROC_1990_204_130_02.
- [13] R. Perry and D. Marshall, 'An Evaluation of Proposed Formula 1 Aerodynamic Regulations Changes Using Computational Fluid Dynamics', in *26th AIAA Applied Aerodynamics Conference*. doi: 10.2514/6.2008-6733.
- [14] J. Newbon, D. Sims-Williams, and R. Dominy, 'Aerodynamic Analysis of Grand Prix Cars Operating in Wake Flows', *SAE International Journal of Passenger Cars - Electronic and Electrical Systems*, vol. 10, pp. 318–329, 2017, [Online]. Available: <https://api.semanticscholar.org/CorpusID:114792565>
- [15] J. J. Newbon, R. G. Dominy, and D. B. Sims-Williams, 'Investigation into the effect of the wake from a generic formula one car on a downstream vehicle', in *The International Vehicle Aerodynamics Conference*, Elsevier, 2014, pp. 213–223. doi: 10.1533/9780081002452.6.213.
- [16] J. Newbon, D. Sims-Williams, and R. Dominy, 'Aerodynamic Analysis of Grand Prix Cars Operating in Wake Flows', *SAE Int. J. Passeng. Cars - Mech. Syst.*, vol. 10, no. 1, pp. 318–329, Mar. 2017, doi: 10.4271/2017-01-1546.
- [17] R. D. Knowles, A. J. Saddington, and K. Knowles, 'On the near wake of a Formula One front wheel', *Proceedings of the Institution of Mechanical Engineers, Part D: Journal of Automobile Engineering*, vol. 227, no. 11, pp. 1491–1502, Nov. 2013, doi: 10.1177/0954407013491903.
- [18] D. Martins, J. Correia, and A. Silva, 'The Influence of Front Wing Pressure Distribution on Wheel Wake Aerodynamics of a F1 Car', *Energies*, vol. 14, no. 15, p. 4421, Jul. 2021, doi: 10.3390/en14154421.
- [19] J. Newbon, R. Dominy, and D. Sims-Williams, 'CFD Investigation of the Effect of the Salient Flow Features in the Wake of a Generic Open-Wheel Race Car', *SAE Int. J. Passeng. Cars - Mech. Syst.*, vol. 8, no. 1, pp. 217–232, Apr. 2015, doi: 10.4271/2015-01-1539.
- [20] M. Watts and S. Watkins, 'Aerodynamic Structure and Development of Formula 1 Racing Car Wakes', *SAE Int. J. Passeng. Cars - Mech. Syst.*, vol. 7, no. 3, pp. 1096–1105, Apr. 2014, doi: 10.4271/2014-01-0600.
- [21] B. Pena and E. Muk-Pavic, 'Biomimetics in Ship Design?', Sep. 2019.
- [22] G. Moscato, J. Mohamed, and G. P. Romano, 'Improving performances of biomimetic wings with leading-edge tubercles', *Exp Fluids*, vol. 63, no. 9, p. 146, Sep. 2022, doi: 10.1007/s00348-022-03493-8.
- [23] J. B. R. Rose, S. G. Natarajan, and V. T. Gopinathan, 'Biomimetic flow control techniques for aerospace applications: a comprehensive review', *Rev Environ Sci Biotechnol*, vol. 20, no. 3, pp. 645–677, Sep. 2021, doi: 10.1007/s11157-021-09583-z.
- [24] M. W. Lohry, D. Clifton, and L. Martinelli, 'Characterization and Design of Tubercle Leading-Edge Wings'.
- [25] S. Sangodkar, 'F1 Aerodynamics : Basics with F1 CFD Models & Jobs in F1', Udemy. Accessed: Aug. 14, 2024. [Online]. Available: <https://www.udemy.com/course/formula-1-aerodynamics/>
- [26] F. Menter, M. Kuntz, and R. Langtry, 'Ten years of industrial experience with the SST turbulence model', *Heat and Mass Transfer*, vol. 4, Jan. 2003.
- [27] F.-J. Granados-Ortiz, P. Morales-Higueras, and J. Ortega-Casanova, '3D CFD simulation of the interaction between front wheels&brake ducts and optimised five-element F1 race car front wings under regulations', *Alexandria Engineering Journal*, vol. 69, pp. 677–698, Apr. 2023, doi: 10.1016/j.aej.2023.02.011.
- [28] Z. Guo, 'Numerical Simulation Study of Drag and Downforce on the Rear Wing of F1 Cars', in *Proceedings of the 2022 2nd International Conference on Computer Technology and Media Convergence Design (CTMCD 2022)*, vol. 99, K. Subramanian, J. Ouyang, and W. Wei, Eds., in *Advances in Computer Science Research*, vol. 99., Dordrecht: Atlantis Press International BV, 2023, pp. 632–645. doi: 10.2991/978-94-6463-046-6_74.
- [29] ferlonso, 'Wingtip Vortices in Formula One - why are they formed?' Accessed: Sep. 02, 2024. [Online]. Available: <https://www.sportskeeda.com/f1/wingtip-vortices-in-formula-one-why-are-they-formed>